Molecules and Cells

Cleavage-Dependent Activation of ATP-Dependent Protease HslUV from *Staphylococcus aureus*

Soyeon Jeong[1], Jinsook Ahn[1], Ae-Ran Kwon[2,*], and Nam-Chul Ha[1,*]

[1]Department of Agricultural Biotechnology, Center for Food Safety and Toxicology, Center for Food and Bioconvergence, and Research Institute for Agriculture and Life Sciences, CALS, Seoul National University, Seoul 08826, Korea, [2]Department of Beauty Care, College of Medical Science, Daegu Haany University, Gyeongsan 38610, Korea
*Correspondence: hanc210@snu.ac.kr (NCH); arkwon@dhu.ac.kr (ARK)
https://doi.org/10.14348/molcells.2020.0074
www.molcells.org

HslUV is a bacterial heat shock protein complex consisting of the AAA+ ATPase component HslU and the protease component HslV. HslV is a threonine (Thr) protease employing the N-terminal Thr residue in the mature protein as the catalytic residue. To date, HslUV from Gram-negative bacteria has been extensively studied. However, the mechanisms of action and activation of HslUV from Gram-positive bacteria, which have an additional N-terminal sequence before the catalytic Thr residue, remain to be revealed. In this study, we determined the crystal structures of HslV from the Gram-positive bacterium *Staphylococcus aureus* with and without HslU in the crystallization conditions. The structural comparison suggested that a structural transition to the symmetric form of HslV was triggered by ATP-bound HslU. More importantly, the additional N-terminal sequence was cleaved in the presence of HslU and ATP, exposing the Thr9 residue at the N-terminus and activating the ATP-dependent protease activity. Further biochemical studies demonstrated that the exposed N-terminal Thr residue is critical for catalysis with binding to the symmetric HslU hexamer. Since eukaryotic proteasomes have a similar additional N-terminal sequence, our results will improve our understanding of the common molecular mechanisms for the activation of proteasomes.

Keywords: ATP-dependent protease, crystal structure, heat shock protein, HslU, HslV, methicillin-resistant *Staphylococcus aureus*, proteasome

INTRODUCTION

Proteasomes in eukaryotic cells are responsible for the active degradation of intracellular proteins conjugated with ubiquitin. Proteasome-dependent protein degradation is essential in the regulation of cellular physiology as well as in amino acid recycling. The cytosolic 26S proteasome consists of a 19S core particle and a 20S regulatory particle (Rousseau and Bertolotti, 2018). The core particle has a proteolytic chamber for protein degradation composed of seven α-type and seven β-type subunits resembling a barrel-shaped cylinder. Three of the seven β-type subunits (β-1, β-2, and β-5) in the core particle belong to the threonine (Thr) protease family, because they employ the N-terminal Thr residue in the mature form as the catalytic nucleophile. The N-terminal 11-72 residues before the Thr residue are processed in their mature forms (Culp and Wright, 2017; Groll et al., 1997; Huber et al., 2016; Thomson and Rivett, 1996).

The bacterial heat shock protein complex HslUV consists of the protease component HslV and the AAA+ ATPase component HslU, which function together as a two-component protease (Chuang et al., 1993; Rohrwild et al., 1996). HslUV is considered a bacterial counterpart of eukaryotic proteasomes because HslV exhibits the highest sequence similarity to the

Received 23 March, 2020; revised 19 May, 2020; accepted 28 June, 2020; published online 22 July, 2020

eISSN: 0219-1032

β-type subunits of eukaryotic proteasomes. To date, HslUV has been most extensively studied in Gram-negative bacteria (Kwon et al., 2003; Sousa et al., 2000; Yoo et al., 1996). Like the eukaryotic β-type subunit of proteasomes, HslV from Gram-negative bacteria belongs to the Thr protease family (Yoo et al., 1997). The catalytic Thr residue (Thr2; numbering is based on the open reading frame sequence in this study) of *Escherichia coli* HslV becomes the first N-terminal residue of the protein because the initiating N-formyl-methionine (Met) is removed during translation (Seemuller et al., 1995; Yoo et al., 1997). The complex structure of *E. coli* HslUV consists of three or four stacked rings, where each ring exhibits a homohexameric arrangement. HslV forms the central two rings of the HslUV complex, and HslU forms a ring at one or both ends. HslU is responsible for recognizing and translocating the substrates using ATP into the central hole of two hexameric rings of HslV. In the purified HslUV complex, HslU substantially stimulated the protease activity of HslV in an ATP-dependent manner (Sousa et al., 2000).

HslUV from *Leptospira interrogans* contributes to its intracellular survival by degrading aggresomes that are generated during infection of host cells (Dong et al., 2017). However, little is known about the cellular functions and substrates of HslUV in most bacteria. In many HslUV biochemical studies, SulA, a cell division inhibitory protein, has been employed as a surrogate proteinaceous substrate (Kanemori et al., 1999). As a colorimetric substrate, benzyloxycarbonyl-Gly-Gly-Leu-7-amino-4-methylcoumarin peptide (Z-GGL-AMC) has been widely used (Rohrwild et al., 1996).

Among Gram-positive bacteria, CodWX (previously known as HslUV) of *Bacillus subtilis* has been studied (Kang et al., 2001). CodW is an HslV-like protease, and CodX is an AAA+ ATPase subunit, the HslU counterpart. CodW has an additional N-terminal sequence before the Thr residue that aligns to the N-terminal Thr2 of *E. coli* HslV; this is similar to the eukaryotic β-type protease component. In the crystal structure of CodW, the additional N-terminal sequence was observed in a symmetric hexameric arrangement similar to that in the *E. coli* HslV oligomeric structure (Fig. 1) (Rho et al., 2008). A previous biochemical study showed that a serine (Ser) residue in the N-terminal extension region was essential for proteolytic activity rather than the Thr residue, and thus it was classified as a member of the Ser protease family (Kang et al., 2001). The crystal structure of a chimeric complex consisting of *B. subtilis* CodW and *E. coli* HslU was determined at 4.16 Å resolution and showed the typical architecture ($U_6V_6V_6U_6$) observed in HslUV complexes of *E. coli* and *Haemophilus influenzae* (Wang et al., 2005).

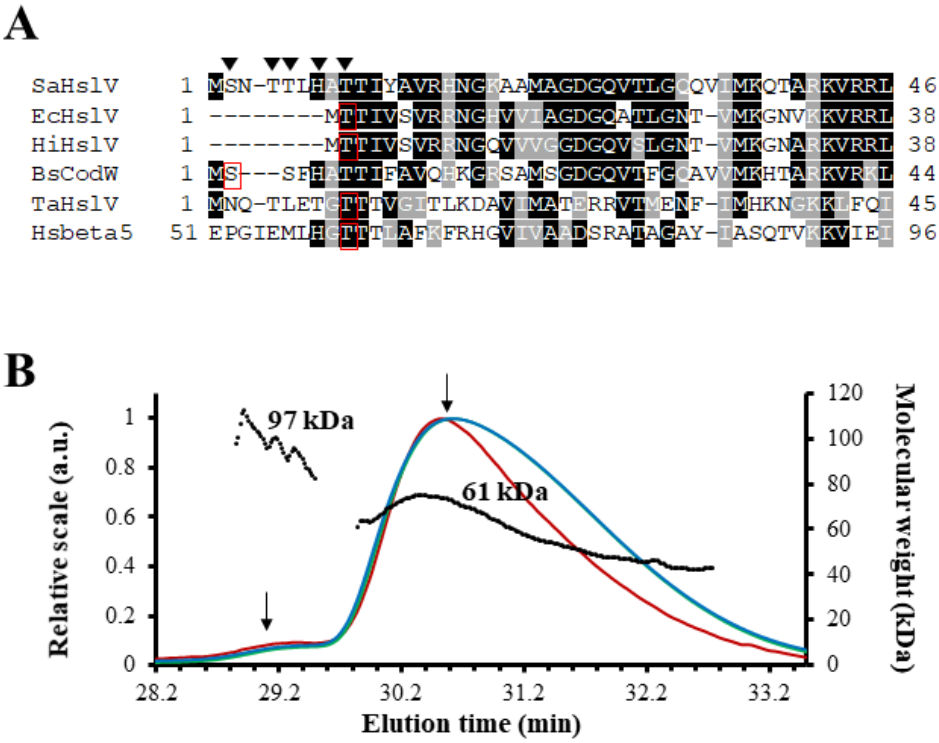

Fig. 1. Features of the SaHslV sequence and oligomeric state. (A) Sequence alignments of HslV homologs around the catalytic Thr residue. The sequence of SaHslV was compared and aligned with HslV from *E. coli* (EcHslV), *H. influenza* (HiHslV), and *T. acidophilum* (TaHslV), CodW from *B. subtilis* (BsCodW), and proteasome β-5 subunit from *Homo sapiens* (Hsβ5) using T-Coffee (Notredame et al., 2000) and the Box Shade server. The red boxes represent the catalytic residues, and the black inverted triangles indicate the mutation sites used in this study. (B) The oligomeric state of the purified SaHslV protein. The protein was analyzed by SEC-MALS using a Superdex 200 10/300 GL (GE Healthcare) column. The signals from ultraviolet (UV; green), refractive index (RI; blue), and light scattering (red) are plotted as solid lines at relative scales (the primary y-axis). The UV and RI lines are overlapped. The molecular weights of the peaks (arrows) are represented by black dots (the secondary y-axis).

The Gram-positive bacterium *Staphylococcus aureus* is a major human pathogen that causes many human diseases and can be fatal, especially when it acquires antibiotic resistance (Hiramatsu et al., 2001). *S. aureus* HslUV (also known as ClpYQ) was implicated in survival under heat-stress conditions, showing functional redundancy with the ClpP proteolytic complex (Chuang et al., 1993). However, its biochemical and structural characteristics remain unknown. Here, we determined the crystal structures of HslV in different states and HslU from *S. aureus*. We further investigated the activation mechanism of the complex in comparison with other proteases, extending our understanding of proteasomes at the molecular level.

MATERIALS AND METHODS

Construction, protein expression, and purification

The gene encoding HslV (National Center for Biotechnology Information reference sequence: BAB57415.1) was polymerase chain reaction-amplified from genomic DNA of *S. aureus* Mu50 and inserted into the pLIC-His vector (Cabrita et al., 2006). The resulting pLIC-HslV construct had 17 additional residues (MHHHHHHENLYFQGAAS) that encoded an N-terminal hexahistidine tag and a TEV cleavage site. pLIC-HslV was transformed into *E. coli* BL21 (DE3) cells, which were cultured in Luria-Bertani broth to express HslV. The protein was induced by the addition of 0.5 mM IPTG. The cells were harvested by centrifugation and resuspended in lysis buffer containing 20 mM Tris-HCl (pH 8.0), 150 mM NaCl, and 2 mM β-mercaptoethanol. After cell disruption by sonication, cell debris was removed by centrifugation. Ni-NTA agarose resin (Qiagen, Germany) was used for the initial purification. The protein-bound resin was eluted with lysis buffer supplemented with 250 mM imidazole. The recombinant TEV protease was treated to cleave the hexahistidine tag in the pooled fractions and then further purified with an anion exchange chromatographic column by applying a gradient of 1 M NaCl. For the final purification step, a gel filtration chromatographic column (HiLoad 16/60 Superdex 200; GE Healthcare, USA) was used with size exclusion chromatography (SEC) buffer (20 mM Tris-HCl buffer (pH 8.0), 100 mM NaCl, 5 mM $MgCl_2$, 0.5 mM EDTA, and 2 mM β-mercaptoethanol). The fractions were concentrated to ~15 mg/ml using a centrifugal membrane concentrator (Vivaspin 20 30,000 MWCO; Sartorius, Germany) and stored at −80°C until use. For HslU, the construction, expression, and puri-

Table 1. X-ray diffraction data

	Twisted SaHslV	Symmetric SaHslV	SaHslU
Data collection			
Beam line	PAL7A	PAL5C	PAL5C
Wavelength (Å)	0.97933	0.97960	0.97960
Space group	$P3_2$	$I222$	$P2_1$
Cell dimensions			
a, b, c (Å)	94.3, 94.3, 227.4	95.6, 108.7, 122.9	146.5, 189.5, 215.6
α, β, γ (°)	90, 90, 120	90, 90, 90	90, 93, 90
Resolution (Å)	50.0-2.00 (2.03-2.00)	50.0-2.33 (2.37-2.33)	50.0-3.00 (3.05-3.00)
R_{merge}	0.076 (0.453)	0.070 (0.351)	0.052 (0.619)
R_{pim}	0.028 (0.260)	0.021 (0.184)	0.032 (0.255)
I/σ_I	17.65 (2.3)	24.5 (2.5)	19.06 (1.96)
Completeness (%)	98.6 (96.6)	98.6 (90.7)	93.1 (87.4)
Redundancy	6.5 (3.6)	8.7 (3.9)	6.2 (5.7)
Refinement			
Resolution (Å)	33.2-2.0	41.3-2.3	36.4-3.0
No. of reflections	125,784	25,104	212,267
R_{work}/R_{free}	0.215/0.264	0.229/0.2856	0.2349/0.2792
No. of total atoms	16,581	4,060	57,793
Wilson B-factor (Å)	31.8	35.15	50.0
R.M.S deviations			
Bond lengths (Å)	0.002	0.003	0.002
Bond angles (°)	0.397	0.600	0.51
Ramachandran plot			
Favored (%)	96.9	96.67	96.60
Allowed (%)	3.1	3.3	3.37
Outliers (%)	0.00	0.00	0.03
PDB code	6KR1	6KUI	6KWW

Numbers in parentheses indicate the statistics for the last resolution shell.
$R_{merge} = \Sigma_{hkl}\Sigma_i|I_i(hkl) - [I(hkl)]|/\Sigma_{hkl}\Sigma_i I_i(hkl)$, where $I_i(hkl)$ is the intensity of the *i*th observation of reflection *hkl* and [I(*hkl*)] is the average intensity of *i* observations.
$R_{p.i.m.} = \Sigma_{hkl}\,[1/(n-1)]^{1/2}\,\Sigma_i|I_i(hkl) - [I(hkl)]|/\Sigma_{hkl}\Sigma_i I_i(hkl)$. R_{pim} is the precision-indicating (multiplicity-weighted) R_{merge}.
R.M.S deviations, root mean square deviations.

fication procedures were performed as reported previously (Jeong et al., 2018).

Crystallization and structural determination

The $P3_2$ crystal form of SaHslV (unprocessed form) was obtained at 14°C within a week by the hanging-drop diffusion method under a reservoir solution containing 0.1 M HEPES sodium (pH 7.5) and 1.5 M lithium sulfate monohydrate. The *I222* crystal form of SaHslV (processed form) was obtained in a mixture with SaHslU at a 1:1 molar ratio and 1 mM ATP after 1 month by the hanging-drop diffusion method under a reservoir solution containing 90 mM Bis-Tris propane, 10 mM citric acid, and 10% polyethylene glycol (molecular weight [MW] 3,350 Da). The SaHslU crystallization condition was described previously (Jeong et al., 2018). The datasets were collected on an ADSC Quantum Q270 CCD detector in beamline 5C at Pohang Accelerator Laboratory, Republic of Korea, at a wavelength of 0.97934 (Hong et al., 2019; Kim et al., 2019). The HKL-2000 program was used to process, merge, and scale the diffraction datasets (Otwinowski and Minor, 1997). The structures were determined by molecular replacement using the CCP4i program (Winn et al., 2011). The SaHslV $P3_2$ and *I222* structures and SaHslU were refined using the PHENIX program (Liebschner et al., 2019) against the final dataset at 2.0 Å, 2.3 Å, and 3.0 Å resolutions, respectively. The Protein Data Bank (PDB) accession code and the details of the datasets are given in Table 1. The refined structures were visualized using PyMOL (Schrödinger, 2010) and Chimera (Pettersen et al., 2004).

Protease assays

The enzymatic assays of HslUV were performed at 25°C in 100-μl reaction mixtures containing 100 μM substrate Z-GGL-AMC (Sigma-Aldrich, USA), 10 μM HslV and/or HslU in SEC buffer, and 1 mM ATP. Degradation of the substrate was measured based on the fluorescence from the liberated AMC at excitation and emission wavelengths of 380 nm and 460 nm, respectively (Rohrwild et al., 1996).

Isolation of the SaHslUV complex

The SaHslUV complex was pre-incubated in SEC buffer in the presence or absence of 1 mM ATP for 30 min at room temperature, and then each sample was loaded onto an SEC column (Superdex 200 increase 10/300 GL; GE Healthcare). The first peak was collected, and each fraction of the first peak was re-subjected to SEC with and without 1 mM ATP in SEC buffer.

SEC-multiangle light scattering (MALS)

SaHslV and SaHslU were prepared with 100 μl of 2 mg/ml protein sample in SEC buffer with and without 1 mM ATP or ADP. Each sample was subjected to SEC on a Superdex 200 increase 10/300 GL column (GE Healthcare). The molecular sizes and oligomerization states of the complexes were measured by MALS (DAWN HELIOS II; Wyatt Technology, USA).

N-terminal sequencing analysis of the SaHslV protein

The purified protein complex from SEC in the presence of 1 mM ATP was subjected to 4%-20% gradient sodium dodecyl sulfate-polyacrylamide gel electrophoresis (SDS-PAGE) (Bio-Rad, USA) and the protein bands were blotted onto a PVDF membrane (GE Healthcare) in a buffer containing 10 mM CAPS (pH 11.0) and 20% methanol. After staining with Coomassie Brilliant Blue R-250, the shorter HslV band was cut from the membrane and subjected to N-terminal amino acid sequence analysis by Proteinworks (Korea) using Edman degradation.

Accession numbers

The atomic coordinates and structure factors (codes 6KR1, 6KUI, and 6KWW) have been deposited in the Protein Data Bank (http://wwpdb.org/).

RESULTS

The lower oligomeric propensity of SaHslV

We performed a sequence alignment with HslV protein from *S. aureus* (SaHslV) and its homologs from Gram-negative bacteria *E. coli* and *H. influenzae*, Gram-positive bacterium *B. subtilis*, archaeon *Thermoplasma acidophilum*, and human proteasome β-5 subunit. The sequence comparison revealed that the conserved Thr residue is in different positions in the various amino acid sequences (Fig. 1A) (Supplementary Fig. S1). While the Thr residue is at the second position in HslV from Gram-negative bacteria, those of the archaeal and human HslV homologs are at the 9th and 60th positions, respectively (Fig. 1A). Removal of the initiator formyl-Met residue was required for proteolytic activity of HslV from Gram-negative bacteria and CodW from *B. subtilis* (Kang et al., 2001). Processing of the N-terminal region before the conserved Thr residue was required for the activation of the archaeal and eukaryotic HslV homologs (Kang et al., 2001). Thus, it was not easy to predict what N-terminal processing is required for the activation of SaHslV from the sequence alignment alone.

We first characterized the oligomeric properties of SaHslV, which are essential for the function of the complex. The oligomeric state of SaHslV in solution was measured with the purified protein (the calculated monomer size is ~20 kDa) by SEC-MALS. The results indicated that SaHslV failed to form a stable hexameric ring arrangement since it mostly behaved as a trimer (~61 kDa) with a minor portion of a higher oligomer (Fig. 1B). This was different from the results of HslV from *E. coli*, which formed a stacked hexameric double-ring structure under similar experimental conditions (Bochtler et al., 1997; Yoo et al., 1996). Thus, our findings showed that SaHslV has a lower propensity to create a hexameric arrangement than *E. coli* HslV, suggesting that the activation mechanism might be different from *E. coli* HslV.

Twisted hexameric structure of SaHslV

To examine the structural features of SaHslV, we determined a crystal structure of the SaHslV protein at 2.0 Å resolution. The asymmetric unit contained 12 protomers displaying the typical stacked double hexameric ring arrangement observed in *E. coli* HslV (Fig. 2A) (Bochtler et al., 1997). However, three distinct conformations (groups A, B, and C) were observed in these protomers in the β-hairpin motif (see below for detail)

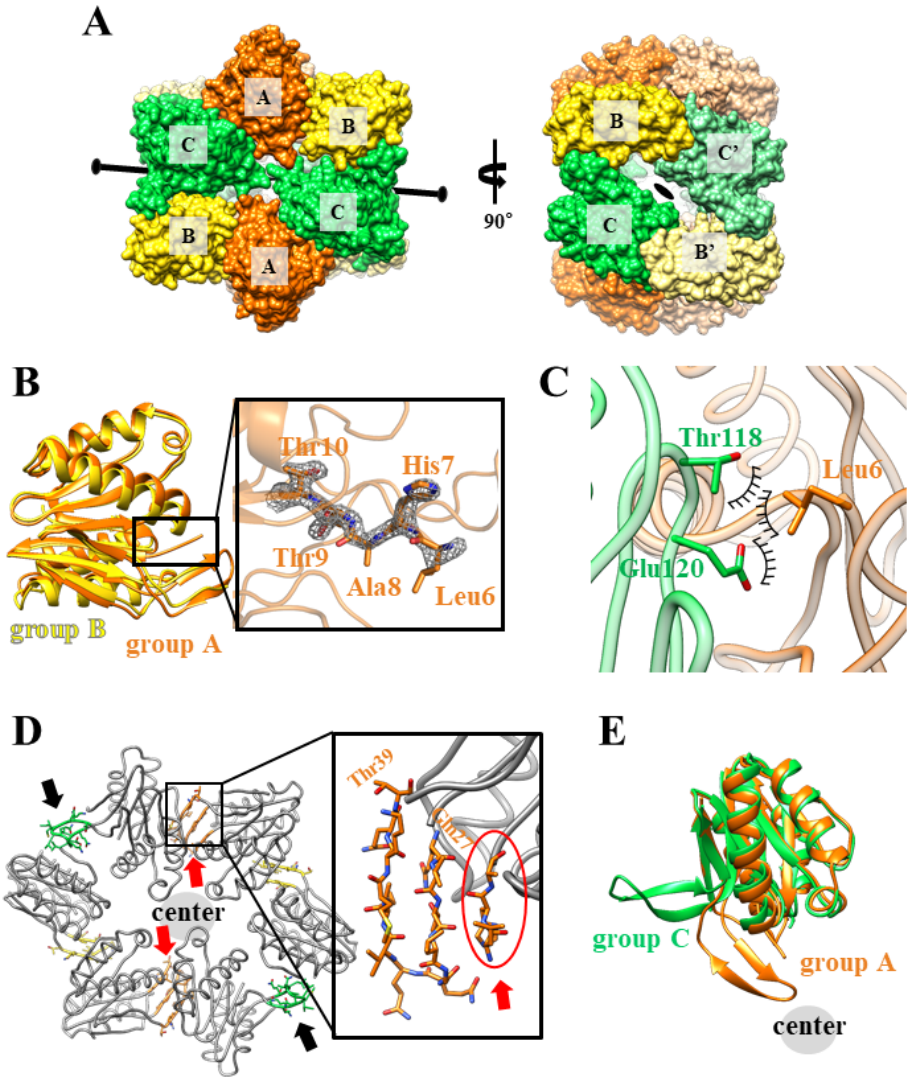

Fig. 2. Structure of the full-length SaHslV protein in the two twisted hexamers. (A) The crystal structure of the full-length SaHslV protein in the doubly stacked hexameric ring arrangement is shown in the surface representations. Twelve protomers are classified into three groups (groups A, B, and C) and each group is colored differently (orange, yellow, and green). The hexamers at the front face and the other face are distinguished by an apostrophe in the label. The (pseudo) two-fold axis is shown. (B) Structure superposition of a group A protomer on a group B protomer. A close-up view of the squared region is shown in the right box. The electron density map (2FoFc, grey) of the additional N-terminal sequence in the group A protomer, contoured at 2.0 sigma, is shown with the stick representation. (C) The interaction of a group C protomer (green) with the N-terminal Leu6 residue in the group A protomer (orange). The contacts between Thr118 and Gln120 from the group A protomer and Leu6 from the group A protomer are shown as spoked arcs. (D) Conformational diversity of the β-hairpin motif (residues Gln27-Thr39) and its interaction with the additional N-terminal sequence. The outward conformation of the β-hairpin motif is shown in green, and the inward conformation is in orange. The additional N-terminal sequence is also in orange and indicated by the red arrows and/or the red circle, which interacts with the β-hairpin motif in the same protomer. The center of the hexameric assembly is marked by a label. The black arrows represent the sites that do not form grooves due to the outward conformation of the β-hairpin motif. (E) Structural superposition between the conformations of the β-hairpin motifs in the protomers of groups A and C. The center of the hexameric assembly is labeled.

at an inter-protomer interface; this is in contrast to the typical hexamers of HslV that show a single conformation of the protomers (Bochtler et al., 1997; 2000; Wang et al., 2001). Due to the different conformations of the protomers, the SaHslV hexameric structure appeared distorted. On the upper side of the dodecamer, the two protomers on the opposite side of the hexamer were in the same conformation. The (pseudo) two-fold axis was between the two hexamers passing through the space between the two group C protomers. Strikingly, the (pseudo) two-fold axis created a large gap between the group C protomers that was larger than the holes in the center of the hexamer (Supplementary Fig. S2).

The conformations of the group A and B protomers are similar to those of *E. coli* HslV (Supplementary Fig. S3) (Baytshtok et al., 2016). However, three additional N-terminal residues (Leu6-His7-Ala8) are observed in the group A protomers (Fig. 2B). In contrast, the residues are disordered in the electron density maps of the group B and C protomers. This difference seemed to be explained by the interaction between the protomers of groups A and C. The protomer of group C has a β-strand (residues 118-125) that is slightly shifted toward the adjacent group A protomer when compared to group A and B protomers. This shift resulted in a tighter molecular contact of Leu6 in the additional N-terminal sequence with Thr118 and Glu120 of the adjacent protomer (Fig. 2C).

This SaHslV structure also revealed a substantial conformational difference in the regions of the β-hairpin motif (residues 27-39), which may be responsible for the interaction with the main body of the adjacent protomer (Fig. 2D). The β-hairpin motifs of the group A and B protomers are similar to the corresponding region of *E. coli* HslV. The β-hairpin motifs of the group A and B protomers are bent inward toward the center of the hexameric ring, making an intermeshing inter-subunit interaction with the main bodies of the group C and A protomers, respectively. These interactions are similar to those of typical *E. coli* HslV structures, creating grooves on the outside of the intermeshing inter-subunit interaction between the β-hairpin motifs and the main bodies. The grooves were previously characterized to be the binding interface for the C-terminal motif of HslU in the ATP-bound form (Sousa et al., 2000).

By contrast, the β-hairpin of group C is oriented outward from the center of the hexameric ring, which is the opposite of those of groups A and B, and *E. coli* HslV (Fig. 2E). The outward conformation of the β-hairpin motif in the group C protomer made only brief interactions with the group B protomer, leading to the creation of a large gap around the (pseudo) two-fold axis of the dodecamer. Thus, this distorted hexameric (or dodecameric) assembly appeared to prevent the interaction with the symmetric HslU hexameric complex due to the partial absence of the grooves for the HslU interaction. Since the additional N-terminal sequence is involved in the formation of this distorted hexameric assembly, our findings suggest that the additional N-terminal sequence prevents the proper oligomeric assembly of SaHslV suited for making a complex with the HslU component.

Symmetric hexameric structure of SaHslV in the presence of SaHslU

To analyze the structural changes of SaHslV upon complex formation with SaHslU, we attempted to determine the com-

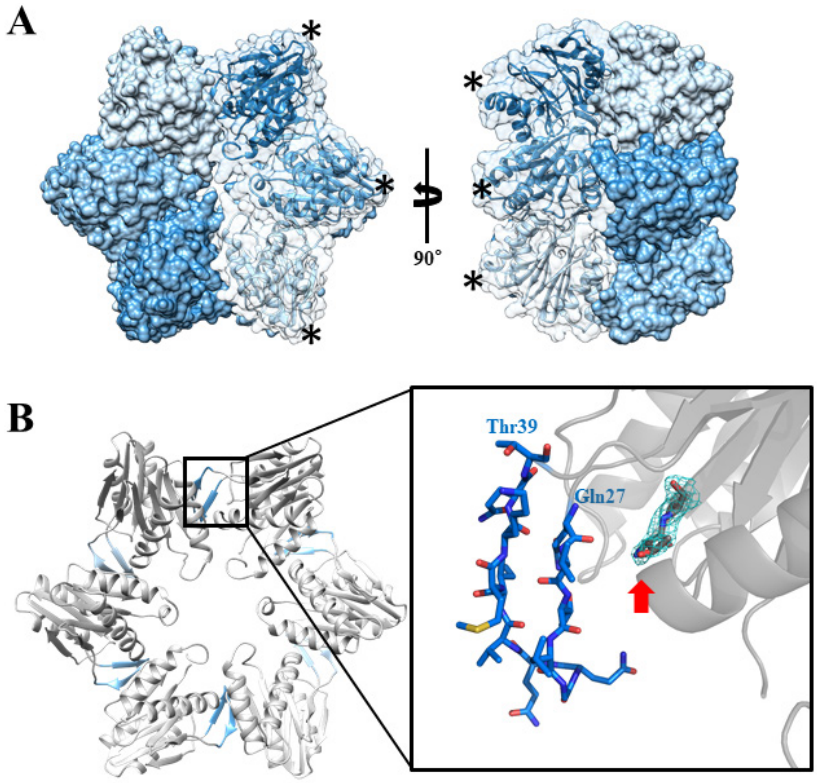

Fig. 3. Crystal structure of the symmetric SaHslV, whose additional N-terminal sequences are cleaved. (A) The HslV structure in the symmetric dodecamer (V_6V_6), which is constructed by applying the 222 symmetry operation with the three protomers in the asymmetric unit (*). The structures are drawn in the surface representations in the orthogonal views. (B) The β-hairpin motifs are shown in blue in the hexamer ring arrangement. A close-up view is shown of the β-hairpin motif, and the red arrow indicates the N-terminal Thr9 residue with its electron density map (cyan).

plex structure of SaHslV and SaHslU with a 1:1 molar ratio of the two proteins in the presence of ATP. However, the crystal contained the SaHslV protein alone, but not the SaHslU protein; overall, this SaHslV structure was similar to the HslV conformation that formed symmetric hexamers, as observed in the dodecameric forms of *E. coli* HslV and *B. subtilis* CodW (Fig. 3A) (Rho et al., 2008; Wang et al., 2001). This symmetric SaHslV structure exhibited substantial structural differences with the twisted hexamer, which might be caused by the prolonged incubation with HslU and ATP during crystallization. This symmetric SaHslV structure did not exhibit the side gaps found in the twisted structure of SaHslV. Since all of the paired β-strands for binding to SaHslU were in the inward conformation filling the side gap of the twisted oligomer, these observations indicated that the symmetric hexamer of SaHslV exhibits the conformation that can form a complex with SaHslU.

Remarkably, the additional N-terminal sequence was not seen in the electron density maps of this symmetric hexamer structure. Thr9 was the first N-terminal residue seen in the electron density maps of all chains of the symmetric HslV structure (Fig. 3B). To identify the actual N-terminal residue of SaHslV in this symmetric HslV structure, we proceeded with the following studies.

SaHslU-dependent processing of the SaHslV N-terminal extension region

Due to the structural differences in the N-terminal region between the twisted and symmetric hexamers, we analyzed the sizes of the proteins by SDS-PAGE. A down-shifted band (a shorter fragment) representing ~20% of the SaHslV protein was generated by incubation with SaHslU and 1 mM ATP. However, a more prolonged incubation did not increase the proportion of the shorter fragment. To identify the actual N-terminal residue of the shorter fragment, we performed N-terminal sequencing analyses of the band by Edman degradation. The shorter fragment of SaHslV started from Thr9 in the N-terminal sequencing analysis, which is in good agreement with the crystal structure of the symmetric SaHslV structure. These results indicated that SaHslV is processed into a shorter fragment with Thr9 as the first N-terminal residue.

To examine whether the ATP hydrolysis is required or just ATP binding is enough for this cleavage of SaHslV, we performed the N-terminal cleavage experiment with non-hydrolysable ATP analogue (AMP-PNP) (Supplementary Fig. S4). As a result, we found that the AMP-PNP activated the HslU-dependent processing of HslV as well as ATP. These results indicate that the ATP binding to HslU, but not ATP hydrolysis, is required for this cleavage at the N-terminal region of HslV.

The processed SaHslV forms a complex with SaHslU for enzymatic activity

We next examined the ability of SaHslV to bind SaHslU. Mixtures of the processed and unprocessed forms of SaHslV with SaHslU in the presence or absence of 1 mM ATP or ADP were subjected to SEC (Fig. 4A). The peak indicating the SaHslUV complex at a larger molecular size appeared only in the presence of ATP. SDS-PAGE analysis of the peak fractions showed that most of the SaHslV in the complex was in the processed form rather than the full-length form. However, the SaHslV in the ADP-containing buffer was not processed and did not form a complex with SaHslU (Supplementary Fig. S5).

To examine the stability of the HslUV complex, we subjected the peak fractions of the complex to SEC in the presence or absence of ATP in the buffer (Fig. 4B). The HslUV complex was intact in the ATP-containing buffer, whereas the complex was dissociated when ATP was absent from the buffer. These results indicate that ATP is required to process SaHslV and to form and maintain the complex with SaHslU (Supplementary Fig. S6).

Proteolytic assays using the synthetic peptide substrate Z-GGL-AMC revealed that only the processed SaHslV in complex with SaHslU was active (Fig. 4C). By contrast, the unprocessed SaHslV did not exhibit proteolytic activity even in the presence of SaHslU and ATP. These results indicate that processed SaHslV, SaHslU, and ATP are indispensable for substrate cleavage by the functional complex. Since the processed and functional SaHslV has a Thr residue at the N-terminus of the protein like typical Thr proteases, it is evident that SaHslV belongs to the Thr protease family, which is different from CodW from *B. subtilis*.

The roles of the N-terminal residues of SaHslV

In the case of *B. subtilis* CodW, Ser2 in the N-terminal extension region plays an essential role in protease activity, which was presented as evidence that CodW is a Ser protease (Kang et al., 2001). To investigate the functions of the Ser, Thr, and His residues in the additional N-terminal sequence of SaHslV in comparison to CodW, we measured the relative protease activities of five N-terminal mutant SaHslV proteins in the presence of SaHslU and 1 mM ATP (Fig. 5). Unlike CodW, the mutation of S2A in SaHslV resulted in only slightly lower activity compared to the wild-type SaHslV. The mutations of T4A/T5A and H7A also showed no critical effects in SaHslV. By contrast, the T9A mutation completely abolished the activity of SaHslV. Since Thr9 is the first N-terminal residue in the processed form, our results support the critical role of Thr9 in the proteolytic activity of SaHslV in complex with SaHslU, which is the hallmark of the Thr protease family.

To examine the processing of the N-terminal regions in the mutant SaHslV proteins, we analyzed the proteins in the presence of SaHslU and ATP by SDS-PAGE. The amount of the processed form of SaHslV (SaHslV* in Fig. 5B) showed a correlation with the relative proteolytic activities of the complex shown in Fig. 5A. Thus, our results indicate that the apparent proteolytic activity represents the processing efficiency of SaHslV, and Thr9 plays a crucial role in the processing of the N-terminal region. Moreover, our results further indicate that Ser2, Thr4, and His7 in the additional N-terminal sequence partly contribute to this N-terminal processing.

Structural features and ATP-dependent proteolytic activity of SaHslU

To examine the structural characteristics of SaHslU, we determined the crystal structure of SaHslU without nucleotides at a resolution of 3.0 Å (Supplementary Fig. S7). The asymmetric unit contained 24 protomers, consisting of two copies of a dodecameric unit (two hexameric rings). The overall structure

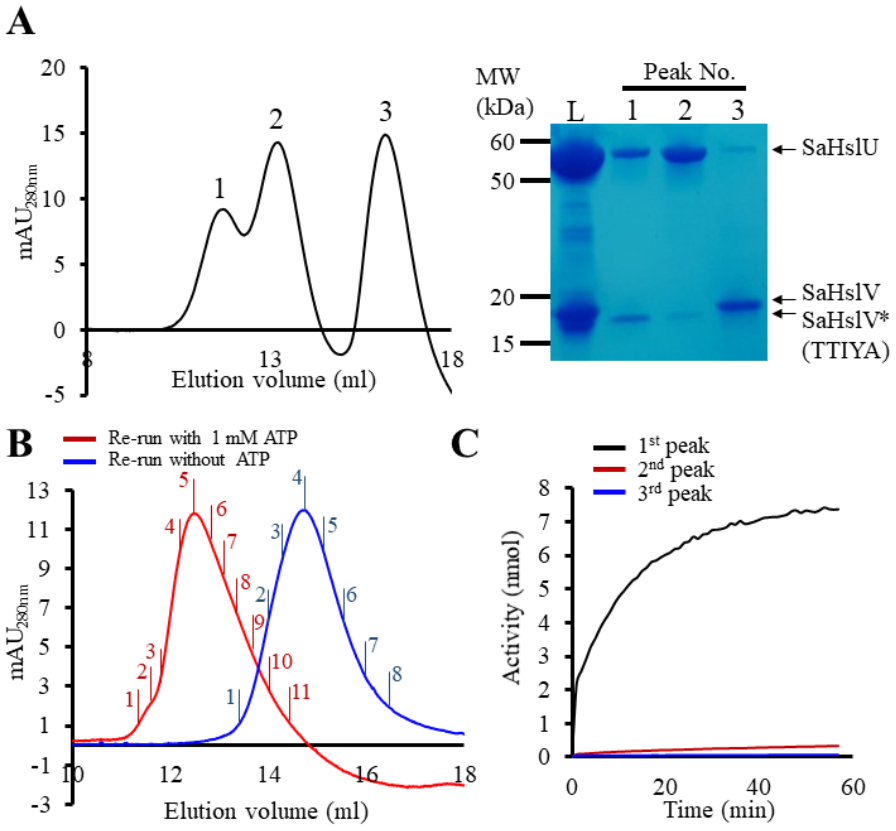

Fig. 4. The N-terminal processing of SaHslV by incubation with SaHslU and ATP. (A) Incubation of SaHslV with SaHslU in the presence of 1 mM ATP for 30 min. The mixture (right, lane L) was loaded into an SEC column. Three peaks are labeled (lanes 1, 2, and 3), and were further analyzed by SDS-PAGE (right, lanes 1, 2, and 3). The expected molecular weights of the peaks based on the elution volumes from the SEC column are shown over the peaks (left). Right, the purified full-length SaHslV protein (HslV) was partly degraded, as shown in lane L, and was isolated by SEC in lanes 1-3. The degraded SaHslV (SaHslV*) was further subjected to Edman degradation N-terminal sequencing, which revealed the sequence TTIYA. (B) ATP-dependent complex formation of SaHslV and SaHslU. Peak 1 in (A), indicating the SaHslUV complex, was re-run in the presence (red line) and absence (blue line) of 1 mM ATP in the buffer. The SDS-PAGE results of the peaks are provided in Supplementary Fig. S6. (C) The proteolytic activities of each peak in (A). The activity of each sample was measured spectrophotometrically based on the liberated AMC from the chromogenic substrate Z-GGL-AMC in 1 mM ATP-containing buffer during 1 h of incubation.

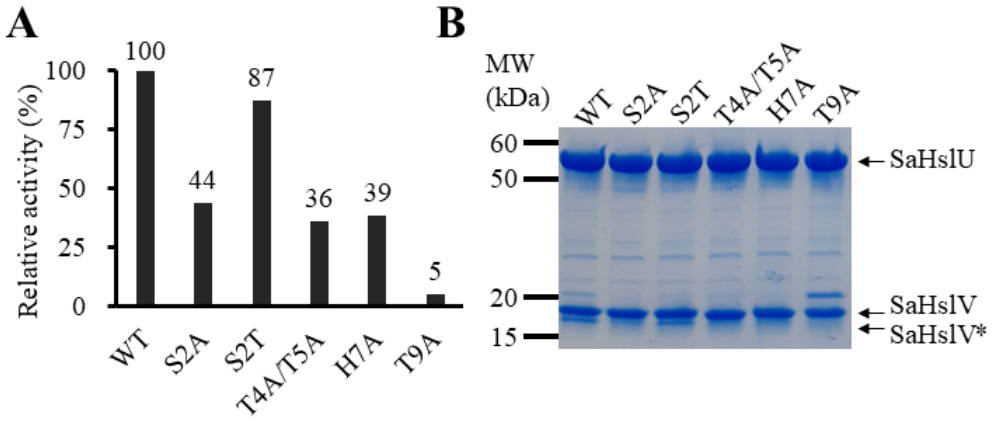

Fig. 5. The proteolytic activities of SaHslUV complexes formed with N-terminal mutant SaHslV proteins. (A) The proteolytic activities of the complexes were measured by the same procedure used in Fig. 4C. The relative activities of the mutant proteins are displayed in comparison with the wild-type protein. (B) The sample was subjected to SDS-PAGE after the 1 h reaction. The shorter fragment (SaHslV*) started from Thr9 in the Edman degradation result.

of the hexameric SaHslU units was similar to those of HslU from *E. coli* and *H. influenzae* (Fig. 6A). SaHslU consists of a nucleotide-binding domain (NBD) containing the Walker A and B motifs for ATP hydrolysis and is flanked by an I domain for the recognition of substrates. The sequence alignment of SaHslU revealed a longer I domain (residues 117-273) (Supplementary Fig. S8). The NBDs were well ordered in the central part of the dodecamer, while the I domain was disordered, mainly at the top and bottom ends of the dodecameric unit (Fig. 6B).

The C-terminal region of HslU only in the ATP-bound form is known to interact with HslV in the complex directly (Bochtler et al., 2000). Thus the conformation of the C-terminal region is essential for binding to HslV. The C-terminal region of SaHslU is folded into the NBD as a short helix in our nucleotide-free structure, which is different from that of HslU from *H. influenzae* in the ATP-bound form (PDB code 1G3I) describing that the corresponding C-terminal region is extended for binding to the HslV component (Sousa et al., 2000). In the SEC-MALS experiments, SaHslU behaved differently in a buffer in the absence of ATP or the presence of ADP (Fig. 6C). SaHslU in the presence of ATP exhibited faster mobility in the SEC column than in the presence of ADP, although the MALS signals indicated that SaHslU forms a hexamer under both conditions. Since the SEC results are affected by the conformation of the protein, our results suggest that SaHslU in the presence of ATP forms a bulkier or more expanded conformation than that in the presence of ADP. The conformational difference of SaHslU might explain the ATP-dependent complex formation with SaHslUV.

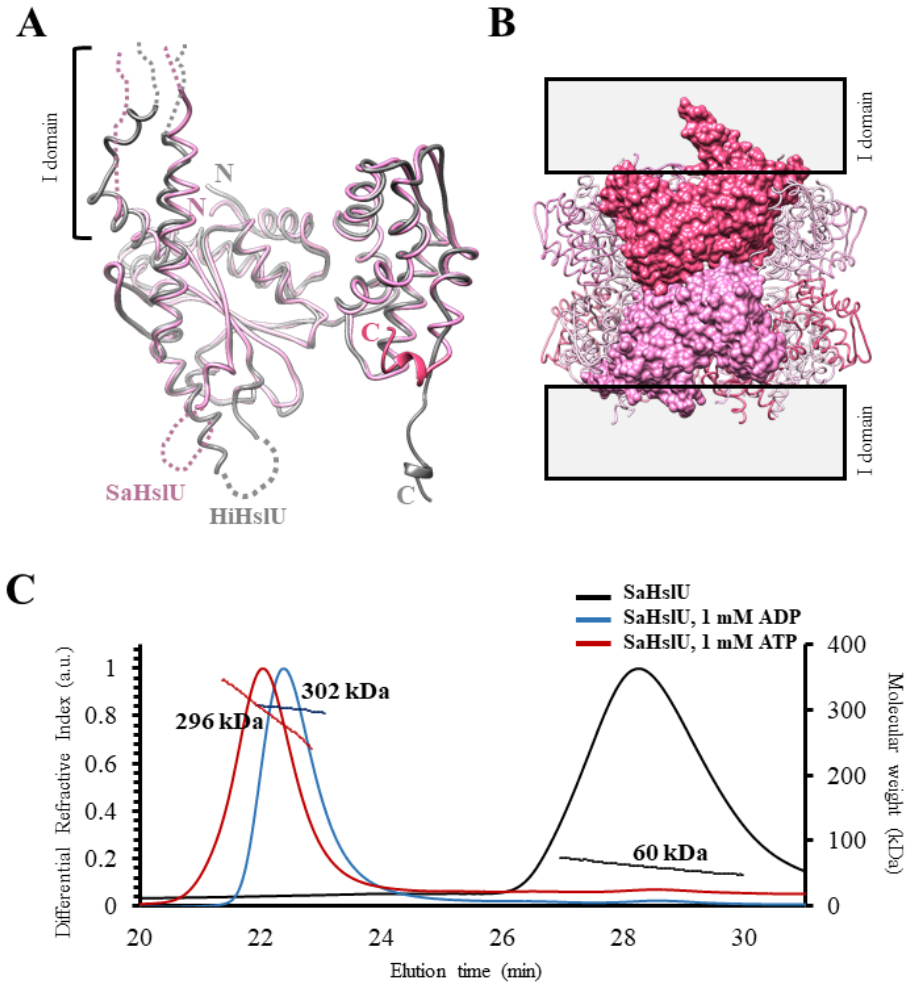

Fig. 6. Structural features of SaHslU. (A) Superposition SaHslU (pink) and *H. influenzae* HslU (gray, PDB code: 1G3I). The dotted line represents the I-domain that is disordered in the crystal structure. The pink and gray arrows point to the C-termini of SaHslU and *H. influenzae* HslU, respectively. (B) Side view of the SaHslU dodecamer. Two protomers are displayed in the surface representations, and the others are in ribbon representations. The gray boxes indicate the I-domains of SaHslU, which are disordered in the crystal structure. (C) Analysis of the SaHslU oligomeric state by SEC-MALS. SaHslU was analyzed in the presence of ATP (red line) and ADP (blue line), and in the absence of nucleotides (black line). The chromatograms show differential refractive index curves with the molecular weights of the peaks calculated by MALS.

DISCUSSION

We determined the crystal structures of SaHslV and SaHslU from the Gram-positive bacterium *S. aureus*. The hexameric structure of the ATPase component SaHslU showed no noticeable difference from those of Gram-negative bacteria. However, the protease component SaHslV exhibited substantial differences in terms of the oligomeric arrangement and activation mechanism when compared to HslV from Gram-negative bacteria. Similar to eukaryotic and archaeal Thr proteases, SaHslV has an additional N-terminal sequence before the catalytic Thr residue, and the additional N-terminal sequence is cleaved when SaHslU and ATP are present. This cleavage leads to the exposure of the Thr residue as the first N-terminal amino acid, which is characteristic of the Thr protease family, triggering the activation of protease activity. Further mutational studies confirmed that SaHslV belongs to the Thr protease family, unlike the Ser protease CodW from *B. subtilis*.

Prokaryotic HslV proteases were believed to be activated by removing only the N-terminal formyl-Met residue. Given the sequence similarity to CodW from *B. subtilis*, SaHslV was expected to show catalytic activity with the Ser2 residue. However, SaHslV exhibited many structural and biochemical properties that are distinct from *B. subtilis* CodW. Our results suggest that *B. subtilis* CodW plays a different role than *S. aureus* SaHslV, or CodW might undergo cleavage in response to an unknown stimulus.

In this study, we showed that ATP-bound SaHslU was involved in processing the N-termianal extension region of SaHslV. We suggest that the C-terminal binding motifs of SaHslU would be extended out to bind SaHslV for the processing and activation of SaHslV in the presence of ATP. However, we don't believe that only the C-terminal peptide of HslU could promote the processing of SaHslV because two of six grooves for the binding interface for the C-terminal motif of HslU are absent in the twisted form of SaHslV. The proper hexameric arrangement and orientation of the C-terminal motif of SaHslU would be more critical for the binding to the twisted form of SaHslV. Since the processed form of SaHslV is more suitable for binding to the ATP-bound form of SaHslU, the binding between the C-terminal motif of SaHslU and SaHslV would be mutually cooperative with the processing of SaHslV. The further complex structure of SaHslU and SaHslV would be required to gain the structural explanation of the cooperative activation of SaHslV.

Although this study demonstrated the SaHslU-dependent cleavage of the additional N-terminal sequence of SaHslV is required for protease activity, only a small portion of SaHslV was cleaved under our experimental conditions. We speculate that other factors or stimuli increase or trigger the cleavage and activation of SaHslV in collaboration with SaHslU. Further study is necessary to identify these factors or stimuli, which will provide insight into the cellular roles of HslUV in the bacteria.

Eukaryotic and archaeal protease components undergo autoprocessing of the additional N-terminal sequence to activate protease activity. In this respect, the activation mechanism of SaHslV requiring SaHslU and ATP is similar to the autolysis-dependent activation of the β-5 subunit in the yeast 26S proteasome. The structure of the yeast β-5 subunit, which is catalytically active, suggests that six residues, Thr1, Asp17, Lys33, Arg19, Ser129, and Asp166 (numbering is based on the matured structure), are involved in autolysis-dependent activation (Huber et al., 2016). Of these, Thr1, Asp17, Lys33, and Ser129 of the yeast β-subunit align with Thr9, Asp25, Lys42, and Ser133 of SaHslV, respectively, in the structural superposition (Supplementary Fig. S9). The residues of the yeast β-5 subunit were better matched to the processed form of SaHslV (Supplementary Fig. S9A) than to the unprocessed structures of SaHslV (Supplementary Figs. S9B-S9D). These findings suggest that the structural change of SaHslV by SaHslU is required for the correct alignment of the residues for autolysis.

This study revealed the overall similarities of SaHslV to eukaryotic proteasomes in terms of the activation by N-terminal processing. However, the detailed activation mechanisms and triggers are still unclear in both SaHslV and eukaryotic proteasomes. Thus, identifying the stimuli that trigger cleavage of the N-terminal extension region will provide important clues about the cellular functions of SaHslUV complex-like Thr proteases. Determining the detailed activation mechanisms and functions of the SaHslUV complex will also improve our understanding of eukaryotic proteasomes.

Note: Supplementary information is available on the Molecules and Cells website (www.molcells.org).

ACKNOWLEDGMENTS

This work was supported by Korea Institute of Planning and Evaluation for Technology in Food, Agriculture, Forestry (IPET) through Agriculture, Food and Rural Affairs Research Center Support Program, funded by Ministry of Agriculture, Food and Rural Affairs (MAFRA) (grant 710012-03-1-HD120 to N.C.H.), and also was supported by the Bio & Medical Technology Development Program of the National Research Foundation (NRF) funded by the Ministry of Science & ICT (grant NRF-2019M3E5D6063871 to N.C.H.). S.J. was supported by the BK21 Plus Program of the Department of Agricultural Biotechnology, Seoul National University, Seoul, Korea. This work was also supported through the National Research Foundation of Korea (NRF) funded by the Ministry of Education of the Korean government (2017R1D1A1B03033857 to A.R.K.). We used beamlines 5C and 7A at Pohang Accelerator Laboratory (Pohang, Republic of Korea) and the MALS facility at the Korea Basic Science Institute (Ochang, Republic of Korea).

AUTHOR CONTRIBUTIONS

S.J. conceived and performed experiments, wrote the manuscript. J.A. provided expertise and feedback. A.R.K. secured funding and provided expertise and feedback and provide reagents. N.C.H. wrote the manuscript and secured funding and provided expertise and feedback.

CONFLICT OF INTEREST

The authors have no potential conflicts of interest to disclose.

ORCID

Soyeon Jeong https://orcid.org/0000-0002-5746-7117
Jinsook Ahn https://orcid.org/0000-0002-4175-5181
Ae-Ran Kwon https://orcid.org/0000-0003-1361-7141
Nam-Chul Ha https://orcid.org/0000-0003-4813-748X

REFERENCES

Baytshtok, V., Fei, X., Grant, R.A., Baker, T.A., and Sauer, R.T. (2016). A Structurally Dynamic Region of the HslU Intermediate Domain Controls Protein Degradation and ATP Hydrolysis. Structure *24*, 1766-1777.

Bochtler, M., Ditzel, L., Groll, M., and Huber, R. (1997). Crystal structure of heat shock locus V (HslV) from *Escherichia coli*. Proc. Natl. Acad. Sci. U. S. A. *94*, 6070-6074.

Bochtler, M., Hartmann, C., Song, H.K., Bourenkov, G.P., Bartunik, H.D., and Huber, R. (2000). The structures of HsIU and the ATP-dependent protease HslU-HslV. Nature *403*, 800-805.

Cabrita, L.D., Dai, W., and Bottomley, S.P. (2006). A family of *E. coli* expression vectors for laboratory scale and high throughput soluble protein production. BMC Biotechnol. *6*, 12.

Chuang, S.E., Burland, V., Plunkett, G., 3rd, Daniels, D.L., and Blattner, F.R. (1993). Sequence analysis of four new heat-shock genes constituting the hslTS/ibpAB and hslVU operons in *Escherichia coli*. Gene *134*, 1-6.

Culp, E. and Wright, G.D. (2017). Bacterial proteases, untapped antimicrobial drug targets. J. Antibiot. (Tokyo) *70*, 366-377.

Dong, S.L., Hu, W.L., Ge, Y.M., Ojcius, D.M., Lin, X., and Yan, J. (2017). A leptospiral AAA+ chaperone-Ntn peptidase complex, HslUV, contributes to the intracellular survival of *Leptospira interrogans* in hosts and the transmission of leptospirosis. Emerg. Microbes Infect. *6*, e105.

Groll, M., Ditzel, L., Lowe, J., Stock, D., Bochtler, M., Bartunik, H.D., and Huber, R. (1997). Structure of 20S proteasome from yeast at 2.4 A resolution. Nature *386*, 463-471.

Hiramatsu, K., Cui, L., Kuroda, M., and Ito, T. (2001). The emergence and evolution of methicillin-resistant *Staphylococcus aureus*. Trends Microbiol. *9*, 486-493.

Hong, S., Son, B., Ryu, S., and Ha, N.C. (2019). Crystal structure of LysB4, an endolysin from *Bacillus cereus*-targeting bacteriophage B4. Mol. Cells *42*, 79-86.

Huber, E.M., Heinemeyer, W., Li, X., Arendt, C.S., Hochstrasser, M., and Groll, M. (2016). A unified mechanism for proteolysis and autocatalytic activation in the 20S proteasome. Nat. Commun. *7*, 10900.

Jeong, S., Ha, N.C., and Kwon, A.R. (2018). Purification and preliminary analysis of the ATP-dependent unfoldase HslU from the gram-positive bacterium *Staphylococcus aureus*. Biodesign *6*, 96-99.

Kanemori, M., Yanagi, H., and Yura, T. (1999). The ATP-dependent HslVU/ClpQY protease participates in turnover of cell division inhibitor SulA in *Escherichia coli*. J. Bacteriol. *181*, 3674-3680.

Kang, M.S., Lim, B.K., Seong, I.S., Seol, J.H., Tanahashi, N., Tanaka, K., and Chung, C.H. (2001). The ATP-dependent CodWX (HslVU) protease in *Bacillus subtilis* is an N-terminal serine protease. EMBO J. *20*, 734-742.

Kim, S., Kim, S.H., Ahn, J., Jo, I., Lee, Z.W., Choi, S.H., and Ha, N. (2019). Crystal structure of the regulatory domain of MexT, a transcriptional activator of the MexEFOprN efflux pump in *Pseudomonas aeruginosa*. Mol. Cells *42*, 850-857.

Kwon, A.R., Kessler, B.M., Overkleeft, H.S., and McKay, D.B. (2003). Structure and reactivity of an asymmetric complex between HslV and I-domain deleted HslU, a prokaryotic homolog of the eukaryotic proteasome. J. Mol. Biol. *330*, 185-195.

Liebschner, D., Afonine, P.V., Baker, M.L., Bunkoczi, G., Chen, V.B., Croll, T.I., Hintze, B., Hung, L.W., Jain, S., McCoy, A.J., et al. (2019). Macromolecular structure determination using X-rays, neutrons and electrons: recent developments in Phenix. Acta Crystallogr. D Struct. Biol. *75*, 861-877.

Notredame, C., Higgins, D.G., and Heringa, J. (2000). T-Coffee: a novel method for fast and accurate multiple sequence alignment. J. Mol. Biol. *302*, 205-217.

Otwinowski, Z. and Minor, W. (1997). Processing of X-ray diffraction data collected in oscillation mode. Methods Enzymol. *276*, 307-326.

Pettersen, E.F., Goddard, T.D., Huang, C.C., Couch, G.S., Greenblatt, D.M., Meng, E.C., and Ferrin, T.E. (2004). UCSF Chimera--a visualization system for exploratory research and analysis. J. Comput. Chem. *25*, 1605-1612.

Rho, S.H., Park, H.H., Kang, G.B., Im, Y.J., Kang, M.S., Lim, B.K., Seong, I.S., Seol, J., Chung, C.H., Wang, J., et al. (2008). Crystal structure of *Bacillus subtilis* CodW, a noncanonical HslV-like peptidase with an impaired catalytic apparatus. Proteins *71*, 1020-1026.

Rohrwild, M., Coux, O., Huang, H.C., Moerschell, R.P., Yoo, S.J., Seol, J.H., Chung, C.H., and Goldberg, A.L. (1996). HslV-HslU: a novel ATP-dependent protease complex in *Escherichia coli* related to the eukaryotic proteasome. Proc. Natl. Acad. Sci. U. S. A. *93*, 5808-5813.

Rousseau, A. and Bertolotti, A. (2018). Regulation of proteasome assembly and activity in health and disease. Nat. Rev. Mol. Cell Biol. *19*, 697-712.

Schrödinger (2010). The PyMOL Molecular Graphics System, version 1.3r1 (New York: Schrödinger).

Seemuller, E., Lupas, A., Stock, D., Lowe, J., Huber, R., and Baumeister, W. (1995). Proteasome from *Thermoplasma acidophilum*: a threonine protease. Science *268*, 579-582.

Sousa, M.C., Trame, C.B., Tsuruta, H., Wilbanks, S.M., Reddy, V.S., and McKay, D.B. (2000). Crystal and solution structures of an HslUV protease-chaperone complex. Cell *103*, 633-643.

Thomson, S. and Rivett, A.J. (1996). Processing of N3, a mammalian proteasome beta-type subunit. Biochem. J. *315* (Pt 3), 733-738.

Wang, J., Rho, S.H., Park, H.H., and Eom, S.H. (2005). Correction of X-ray intensities from an HslV-HslU co-crystal containing lattice-translocation defects. Acta Crystallogr. D Biol. Crystallogr. *61*, 932-941.

Wang, J., Song, J.J., Franklin, M.C., Kamtekar, S., Im, Y.J., Rho, S.H., Seong, I.S., Lee, C.S., Chung, C.H., and Eom, S.H. (2001). Crystal structures of the HslVU peptidase-ATPase complex reveal an ATP-dependent proteolysis mechanism. Structure *9*, 177-184.

Winn, M.D., Ballard, C.C., Cowtan, K.D., Dodson, E.J., Emsley, P., Evans, P.R., Keegan, R.M., Krissinel, E.B., Leslie, A.G., McCoy, A., et al. (2011). Overview of the CCP4 suite and current developments. Acta Crystallogr. D Biol. Crystallogr. *67*, 235-242.

Yoo, S.J., Seol, J.H., Shin, D.H., Rohrwild, M., Kang, M.S., Tanaka, K., Goldberg, A.L., and Chung, C.H. (1996). Purification and characterization of the heat shock proteins HslV and HslU that form a new ATP-dependent protease in *Escherichia coli*. J. Biol. Chem. *271*, 14035-14040.

Yoo, S.J., Shim, Y.K., Seong, I.S., Seol, J.H., Kang, M.S., and Chung, C.H. (1997). Mutagenesis of two N-terminal Thr and five Ser residues in HslV, the proteolytic component of the ATP-dependent HslVU protease. FEBS Lett. *412*, 57-60.